# Reaction mechanisms in $^{16}O+^{40}Ca$ at an incident energy of $E(^{16}O) = 86$ MeV through inclusive measurements of $\alpha$ and proton spectra

Chinmay Basu,[1] S. Adhikari,[1] S. K. Ghosh,[1] S. Roy,[1] S. Ray,[2,*] B. R. Behera,[3] and S. K. Datta[4]
[1]*Saha Institute of Nuclear Physics, 1/AF Bidhan Nagar, Calcutta 700064, India*
[2]*Physics Department, Kalyani University, Kalyani, West Bengal 741325, India*
[3]*Department of Physics, Panjab University, Chandigarh-160014 (UT), India*
[4]*Inter University Accelerator Center, New Delhi-110067, India*
(Received 28 June 2007; published 24 September 2007)

The $\alpha$ and proton spectra from the $^{16}O+^{40}Ca$ reaction is measured at $E(^{16}O) = 86$ MeV at several laboratory angles between 54° and 138°. Analysis in terms of the statistical model for compound nuclear reactions show that an event-by-event calculation of the evaporation spectra removes discrepancy observed with standard calculations.

DOI: 10.1103/PhysRevC.76.034609 PACS number(s): 21.10.Jx, 23.50.+z

## I. INTRODUCTION

The study of light charged particles emitted in heavy ion reactions can provide interesting information about the reaction mechanism. Simple inclusive measurements along with reaction model analysis can often be sufficient for this purpose. Recently, many studies have investigated the continuous light particle spectra in the light of statistical model calculations for heavy ion induced compound nuclear reactions [1–9]. These calculations with a standard set of parameters fail to reproduce the light particle (especially $\alpha$ particles and protons) experimental spectra. This problem is also found to be dependent on the entrance channel symmetry. The problem is solved if the emitter nucleus is considered to be deformed and the yrast line is modified by a change of the moment of inertia from its rigid body value. However, this solution holds good only for $\alpha$ particle spectra and not for protons. To obtain a good prediction of both $\alpha$ and proton spectra, a dynamical model for fusion has been suggested in Ref. [7] for calculating the maximum angular momentum required as input for the statistical model. Another solution that has emerged [10,11] is to use a structure-dependent level density parameter in the statistical model calculations. However, most of these works used the statistical model code CASCADE [12], which uses two completely arbitrary parameters to modify the yrast line. On the other hand, an event-by-event calculation of the reaction process [13] has been used less frequently for this purpose [14].

In this work, we study the reaction mechanism of the $^{16}O+^{40}Ca$ reaction at 86 MeV incident energy by an inclusive measurement of $\alpha$ and proton spectra. The same system has been studied through the measurement of light particles at projectile energies both above [15,16] and below [17–19] 86 MeV. We also choose this reaction so as to populate the same compound nucleus $^{56}Ni$ at the same excitation energy of 76 MeV, populated by $^{28}Si+^{nat}Si$ reaction, as studied by us in an earlier work [10]. The calculation of the evaporation spectra by an event-by-event basis removes the shortcomings of the standard evaporation calculations.

## II. EXPERIMENTAL DETAILS

The experiment was carried out using the 14UD Pelletron facility of the Nuclear Science Center (presently Inter University Accelerator Center) at New Delhi. The $6^+$ $^{16}O$ beam at 86 MeV was bombarded onto a self-supporting Ca target of thickness 5 mg/cm$^2$. The target was kept in kerosene and was vacuum transported into the target ladder of the general purpose scattering chamber. Standard electronics and a Computer Automated Measurement And Control (CAMAC)-based data acquisition system were used in the experiment. Two detector telescopes ($\Delta E$-$E$) were set up using solid state Si detectors. Measurements were made at both forward and backward angles ranging from 54° to 138°.

## III. RESULTS AND DISCUSSIONS

The measured two-dimensional $\Delta E$-$E$ spectra are shown in Fig. 1. The $Z = 1$ and $Z = 2$ isotopes are nicely separated. The gated one-dimensional spectra for $\alpha$ particles at forward and backward angles are shown in Figs. 2 and 3, respectively. Similarly, the proton spectra are shown in Figs. 4 and 5. The inclusive double differential cross sections are shown at various laboratory angles mentioned in the inset. Since the spectra are measured at angles beyond 54° we do not expect any significant contribution of the breakup of $^{16}O$ into $\alpha$ and $^{12}C$ [20]. Moreover, if the spectra had resulted from projectile breakup, then the expected position of the peak in the $\alpha$ spectra would be at 21.5 MeV. On the other hand, the observed peak for $\alpha$ particles at forward angles is around 10 MeV, and the shape of the spectra is close to a Maxwellian distribution. In Fig. 6, we show the experimental velocity component diagrams for $\alpha$ particles and protons. As can be seen from the figure, the velocities indicate a statistical process with the center at the compound system velocity. Based on the experimental signatures, we analyze the spectra in terms of the statistical model for compound nuclear reactions. A large number of experiments in the recent past [1,2,4–11] that studied light charged particle emissions in heavy ion reactions used the code CASCADE to interpret the reaction mechanism. CASCADE relies on a standard evaporation model using several parameters (two of which are completely arbitrary) to calculate

[*]Present address: Vivekananda University, Belur Math, Howrah, West Bengal, India.

 

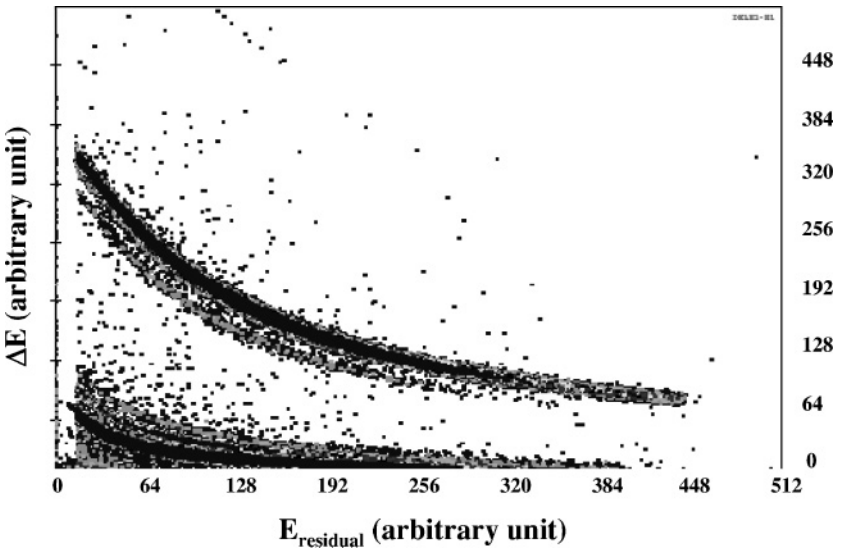


FIG. 1. Two-dimensional $\Delta E$-$E_{\text{residual}}$ spectra at 54°.

the continuous light particle spectra. However, the results from CASCADE have suffered from several problems related to explaining the observed particle spectra. These problems have been resolved mainly through modification of the various input parameters such as the angular momentum [7] or level density parameter [10]. An important aspect in the evaporation calculation is to consider all possible processes in the deexcitation cascade of the mother compound nucleus. For example, the phenomena of multiple emissions include both sequential and simultaneous processes. However, in a standard evaporation calculation such as in CASCADE, the former is taken into account, whereas the latter process is totally ignored because of the additional complexities involved in the formalism for simultaneous emissions. As a result of this incomplete description, the population cross section of particular nuclei in the decay cascade, as a function of excitation energy and angular momentum, may not be properly evaluated. This is clearly evident in Figs. 2 and 3, where the standard evaporation calculations from CASCADE (shown by dotted lines) do not explain the $\alpha$ and proton spectra satisfactorily. To account for the inaccurate description of the population cross section, we calculated the $\alpha$ and proton spectra using the Monte Carlo statistical model code PACE [13]. Before we discuss the results of our calculations, we outline some distinctive features and parameters of the two codes.

### A. Statistical calculations with CASCADE and PACE

In the statistical model, the rate of particle decay from the initial compound nuclear state $i$ to the final residual state $f$ is given as

$$R_p(E_i J_i; E_f J_f)dE = \frac{\rho(E_f, J_f, \pi_f)}{\hbar\rho(E_i, J_i, \pi_i)} \sum_{|J_f - s|}^{J_f+s} \sum_{l=|J_i-S|}^{J_i+S} T_l^p(\epsilon_p)dE, \quad (1)$$

where $\epsilon_p = E_f - E_i - S_p$ is the particle energy, $S_p$ is the particle separation energy, and $s$ is the spin of the particle $p$. In the summation over $l$ the criterion for parity conservation should be included. The level density in the above equation is defined as

$$\rho(E, J, \pm\pi) = \frac{2J+1}{12}\sqrt{a}\left(\frac{\hbar^2}{2\mathcal{I}}\right)^{3/2}\frac{\exp\sqrt{a(E-E_{\text{rot}})}}{(E-E_{\text{rot}})^2}. \quad (2)$$

In the above equation, $E$ is the excitation energy and $E_{\text{rot}} = (\frac{\hbar^2}{2\mathcal{I}})J(J+1)$ is the rotational energy of the nucleus. The moment of inertia $\mathcal{I}$ can be calculated from a rigid body prescription, i.e., $\mathcal{I}_{\text{rigid}} = 2MR^2/5$. The basic difference between CASCADE and PACE lies in the method of calculating the probabilities of different channels (as a function of

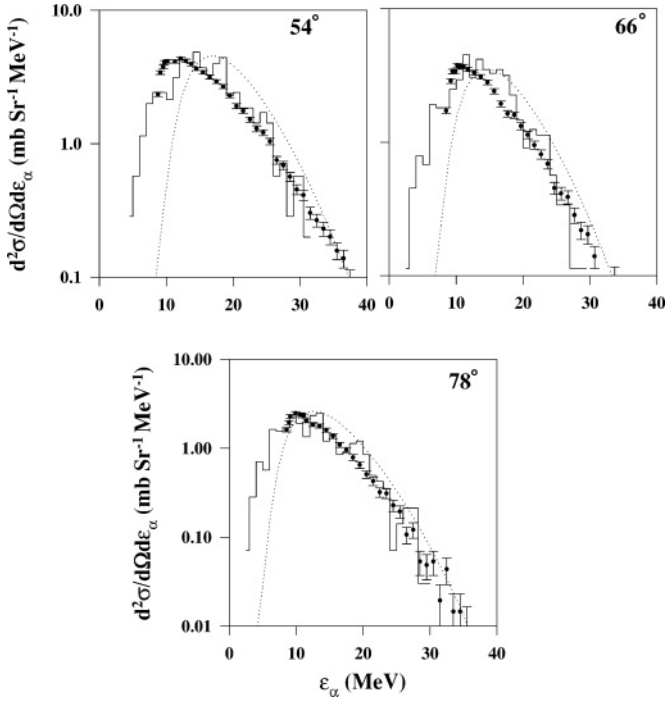


FIG. 2. Measured inclusive double differential $\alpha$ particle cross section (symbols) at different laboratory angles indicated in the inset. Also shown are CASCADE (dotted lines) and PACE (solid lines) calculations with parameters described in the text.

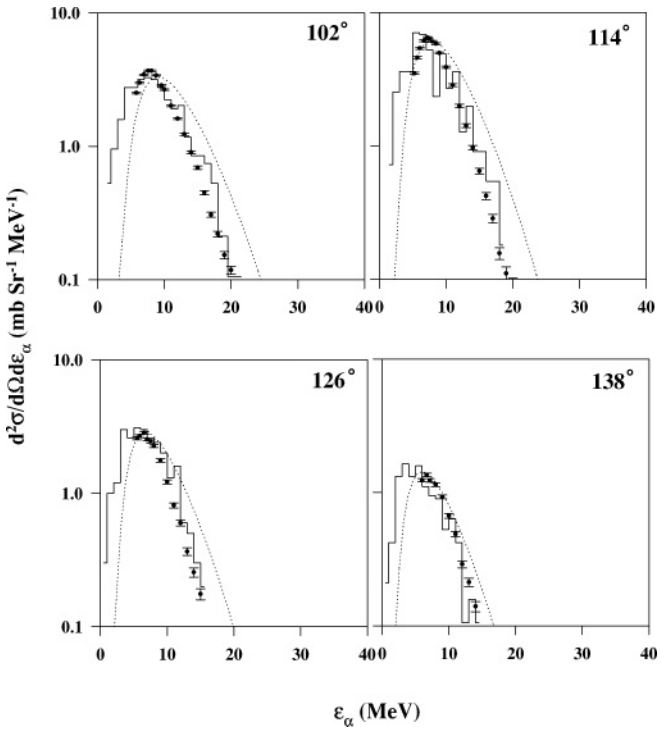


FIG. 3. Same as Fig. 2, except for different laboratory angles.

excitation energy and spin) in the decay chain of the excited nuclei. In PACE, the population of a residual event (evaporation residue formed through evaporation of neutrons, protons, or $\alpha$ particles) is calculated by a Monte Carlo method. When the total number of events are few, the population of different residual nuclei are equally probable. As in the real

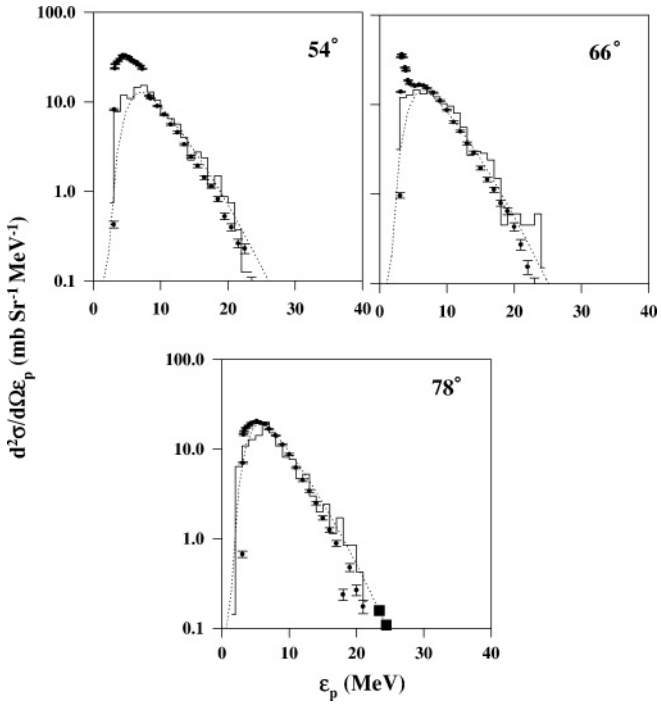


FIG. 4. Same as Fig. 2, except for protons.

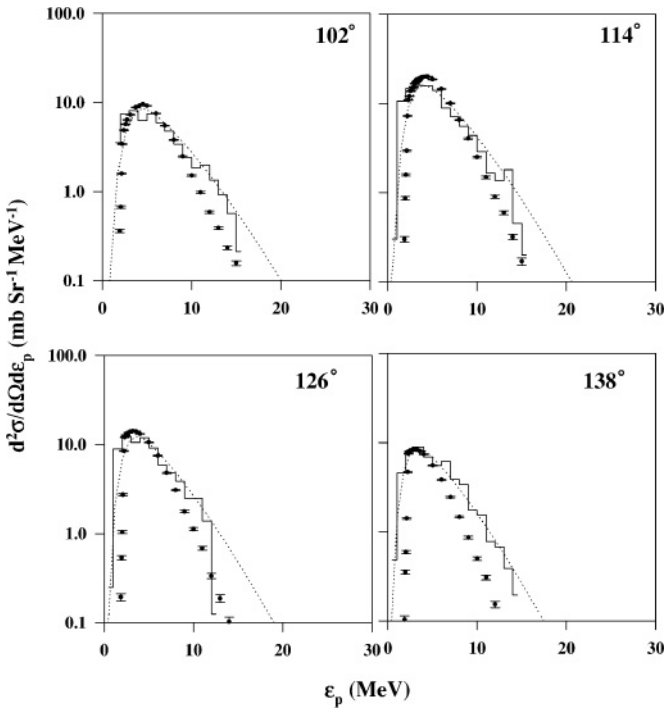


FIG. 5. Same as Fig. 3, except for protons.

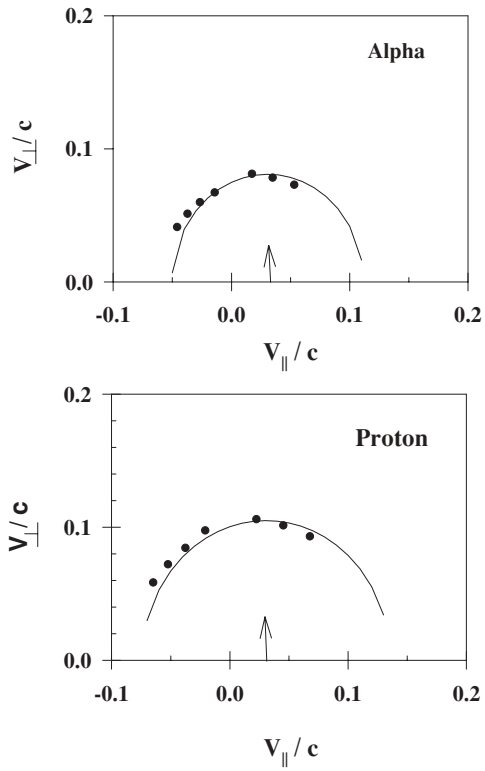


FIG. 6. Velocity diagram for $\alpha$ particles and protons for the present reaction. The arrow indicates the center-of-mass velocity. The solid line represents a circle of radius equal to the average velocity of the particle.

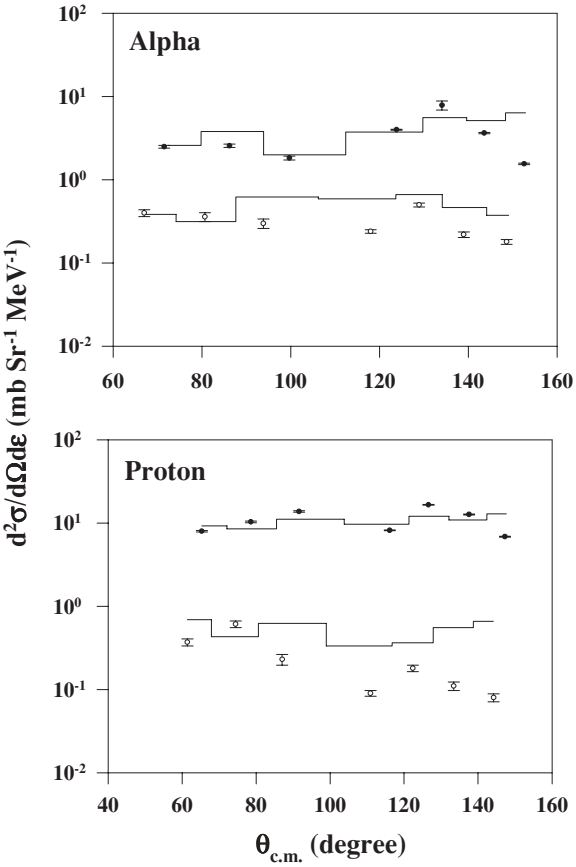


FIG. 7. Center-of-mass angular distributions for $\alpha$ particles with energy bins 12–13 MeV (top) and 22–23 MeV(bottom) and protons with energy bins 7–8 MeV (top) and 17–18 MeV (bottom). The solid lines show the corresponding PACE calculations.

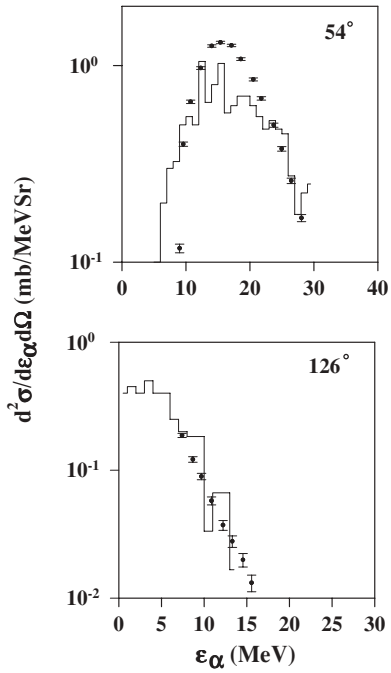


FIG. 8. Representative PACE calculations (solid lines) at 54° and 126° compared with $^{28}$Si+$^{28}$Si data (symbols) of Ref. [10]. The parameters used in the PACE calculations are the same as those for the present system.

situation, there may be a large number of events and then the population is guided purely by random statistics. In the present case, the total number of events considered in the calculation is 5000. An increase in this number does not change the results significantly. Once the population cross section of each residual nucleus is determined, the decay of light particle probability is evaluated from Eq. (1). On the other hand, in CASCADE, the average population cross section of a residual nucleus is calculated from the statistical model. The decay is again obtained from Eq. (1). Thus in PACE, an event-by-event followup of the reaction is possible, whereas in CASCADE an average behavior is assumed. Besides, angular distributions in PACE are calculated from the conservation of angular momentum, whereas in CASCADE, an isotropic angular distribution in the center of mass is considered. Furthermore, shape changes due to rotation are incorporated into CASCADE by a parametrization of the moment of inertia as $\mathcal{I} = \mathcal{I}_{\text{rigid}}(1 + \delta_1 J^2 + \delta_2 J^4)$ in terms of the rigid body moment of inertia and two arbitrary parameters $\delta_1, \delta_2$.

In Figs. 2 and 3, dotted lines show the results of our calculations using CASCADE; and solid lines, using PACE. The laboratory spectra at various angles from CASCADE are obtained by a kinematic conversion of the c.m. spectra with isotropic angular distributions. We have studied earlier [10] the $\alpha$ and proton spectra from the same $^{56}$Ni compound nucleus at an excitation energy ($\approx$76 MeV) but populated through a symmetric channel ($^{28}$Si+$^{\text{nat}}$Si). A comparison with the results of the present work will therefore help us to investigate the possible entrance channel dependence of the statistical model calculations. In an earlier work [5], to remove the entrance channel dependence, the maximum angular momentum for fusion ($l_{\max}$) was calculated from a dynamical model [21]. This model suggests a much smaller $l_{\max}$ for the symmetric channel than that obtained from standard fusion models, such as the Bass model [22]. In the present case, we calculated $l_{\max}$ using the dynamical model code HICOL [21] for both the $^{28}$Si+$^{28}$Si and $^{16}$O+$^{40}$Ca reactions. The values of $l_{\max}$ for both the symmetric and asymmetric reactions predicted by HICOL are almost the same and can be taken as $l_{\max} = 26\hbar$. The other important parameters used in the CASCADE calculations are the level density parameter ($a = A/9$), radius parameter $r_0 = 1.28$ fm, and the sensitive parameters $\delta_1 = 1.2 \times 10^{-4}$ and $\delta_2 = 1.1 \times 10^{-7}$. The optical potential parameters for $\alpha$ and protons are, respectively, adopted from Huizenga-Igo [23] and Perrey [24]. The values of the sensitive parameters $\delta_1, \delta_2$ are kept the same as those for the $^{28}$Si+$^{28}$Si case [10]. In the CASCADE calculations shown in Figs. 2 and 3, we use $l_{\max} = 33\hbar$ (Bass model) along with the above-mentioned parameters. The low energy part is underpredicted with the higher energy overpredictions increasing with increasing backward angles. The use of the HICOL predicted $l_{\max}$ does not improve the agreement of the calculation with the observed spectra. The low energy underpredictions may result from the assumption of a spherical residual nucleus (treated as the target in the calculation of inverse cross sections). A

deformation in this case is usually introduced by increasing the value of $r_0$ [2]. The radius parameter $r_0$ occurring in the rigid body moment of inertia affects the higher energy part of the cross section. We examined the results of our calculations using a value of $r_0 = 1.28$ fm and a calculation with $r_0$ increased by 16% in the optical potential, keeping $r_0$ in the moment of inertia as 1.28 fm. This increase in $r_0$ does not make any appreciable improvement in terms of increments in low energy cross sections. An increase in $r_0$ for both optical potential and moment of inertia, however, worsens the predictions. Low energy underpredictions may also result from insufficient consideration of decay chain residual nuclei and emissions of observed particles therefrom. Since the population of the different residual nuclei populated in the reaction are calculated on an event-by-event basis by PACE, we may expect some improvements in the predicted spectra from this code.

The PACE calculations are shown by solid lines in Figs. 2–5. The best description of experimental data can be achieved with $l_{max} = 33\hbar$, $r_0 = 1.28$ fm, $\delta_1 = 1.2 \times 10^{-4}$, $\delta_2 = 1.1 \times 10^{-7}$, and $a = A/9$. Both the lower energy underpredictions and angular dependence of the higher energy fit are removed in the PACE calculations. The PACE parameters are kept similar to that used in CASCADE except that the rotational energies are calculated from the rotating liquid drop model (RLDM) prescription and without the arbitrary parameters $\delta_1$, $\delta_2$. The overall agreement with the experimental data is found to be more improved by the PACE calculations than by the CASCADE ones, especially for $\alpha$ particles. The $\alpha$ and proton angular distributions in the center-of-mass frame are shown in Fig. 7 along with PACE predictions. An isotropic behavior is observed signifying a compound process. To examine the entrance channel dependence (if any) of the calculations, we analyzed the data of $^{28}Si+^{28}Si$ [10] using PACE with the same set of compound nuclear parameters such as level density parameter, deformability, radius parameter, etc. The maximum angular momentum values were not adjusted in the PACE calculations. The results of the calculations (Fig. 8) are, however, satisfactory for the symmetric channel as well, though $l_{max}$ in this case from the BASS model is different ($l_{max} = 29$) from the asymmetric channel ($l_{max} = 33$) and that predicted by HICOL ($l_{max} = 26$). In the $\alpha$ spectra, we observe an angle dependence in the quality of fit for CASCADE calculations. However, with PACE, the calculations reproduce the data equally well at both forward and backward angles. More systematic analyses of the statistical spectra using PACE could be carried out for a wide range of systems and energies.

## IV. SUMMARY AND CONCLUSIONS

In this work, we have studied $\alpha$ and proton spectra emitted in a heavy ion induced reaction. The dominant reaction mechanism is the compound nuclear process. An event-by-event calculation shows that proper evaluation of the population cross section for various nuclei in the decay cascade is essential to explaining the observed spectra.

## ACKNOWLEDGMENTS

We acknowledge K. S. Golda, V. P. Yogi, the Pelletron staff, IUAC, New Delhi, and the target laboratory, VECC, Kolkata, for their support in this work.

[1] G. Viesti *et al*., Phys. Rev. C **38**, 2640 (1988).
[2] D. Bandyopadhyay *et al*., Eur. Phys. J. A **14**, 53 (2002).
[3] M. Rousseau *et al*., Phys. Rev. C **66**, 034612 (2002).
[4] J. Kaur, A. Kumar, A. Kumar, G. Sing, S. K. Datta, and I. M. Govil, Phys. Rev. C **70**, 017601 (2004).
[5] I. M. Govil, R. Singh, A. Kumar, A. Kumar, G. Singh, S. K. Kataria, and S. K. Datta, Phys. Rev. C **62**, 064606 (2000).
[6] I. M. Govil *et al*., Nucl. Phys. **A674**, 377 (2000).
[7] J. Kaur, I. M. Govil, G. Singh, A. Kumar, A. Kumar, B. R. Behera, and S. K. Datta, Phys. Rev. C **66**, 034601 (2002).
[8] C. Bhattacharya *et al*., Nucl. Phys. **A655**, 841c (1999).
[9] C. Bhattacharya *et al*., Phys. Rev. C **65**, 014611 (2001).
[10] C. Basu *et al*., Int. J. Mod. Phys. E **14**, 1063 (2005).
[11] S. Adhikari *et al*., Phys. Rev. C **74**, 024602 (2006); Eur. Phys. J. A **25**, s01 299 (2005).
[12] F. Pühlhofer, Nucl. Phys. **A280**, 267 (1977).
[13] A. Gavron, Phys. Rev. C **21**, 230 (1980).
[14] B. Fornal *et al*., Phys. Rev. C **44**, 2588 (1991).
[15] J. Brzychczyk *et al*., Phys. Lett. **B194**, 473 (1987).
[16] Y. Chan, M. Murphy, R. G. Stokstad, I. Tserruya, S. Wald, and A. Budzanowski, Phys. Rev. C **27**, 447 (1983).
[17] Tai Kuang-hsi *et al*., Nucl. Phys. **A316**, 189 (1979).
[18] P. Janker *et al*., Eur. Phys. J. A **4**, 147 (1999).
[19] S. Wald, I. Tserruya, Z. Fraenkel, G. Doukellis, H. Gemmeke, and H. L. Harney, Phys. Rev. C **28**, 1538 (1983).
[20] D. C. Slater *et al*., Phys. Rev. Lett. **33**, 784 (1974).
[21] H. Fieldmeir, Rep. Prog. Phys. **50**, 915 (1987).
[22] R. Bass, Nucl. Phys. **A231**, 45 (1974).
[23] J. R. Huizenga and G. Igo, Nucl. Phys. **29**, 462 (1962).
[24] F. G. Perey, Phys. Rev. **131**, 745 (1963).